





Alteration Mineralogy and Fluid Inclusion Microthermometry of the Hes-Daba Area in Gagade, Republic of Djibouti

Ali Ferat Bayram ^{*1}, Moussa Hassanleh Hassan ²

¹ Konya Technical University, Department of Geological Engineering, Turkiye, afbayram@ktun.edu.tr

² Djiboutian Office for The Development of Geothermal Energy, moussaabdi123@gmail.com

Cite this study:

Bayram, A.F. & Hassanleh Hassan, H (2025). Alteration Mineralogy and Fluid Inclusion Microthermometry of the Hes-Daba Area in Gagade, Republic of Djibouti. *International Journal of Engineering and Geosciences*, 9 (1), 79-86.

<https://doi.org/10.31127/tuje.1509702>

Keywords

Hes-Daba,
Gagade,
Hanle,
Republic of Djibouti,
Fluids inclusions

Research Article

Received:3.07.2024
Revised: 19.08.2024
Accepted:22.08.2024
Published:20.01.2025



Abstract

This study focuses on fluid inclusions from the Hes-Daba area. Microthermometric measurements were conducted on quartz collected from surface veins that hosted inclusions in two phases: liquid and vapor. The mean homogenization temperature ranged from 150 °C to 367 °C and the melting point of ice ranged from -0.05 °C to -1.14 °C, indicating that the inclusion solutions consisted of 0.1 to 1.9 eq. wt% NaCl. The thermal history and thermal structure were evaluated to estimate the formation temperature. Selected samples were analyzed via x-ray diffraction to provide direct data on geothermal reservoirs; this was necessary because geothermal fluids, through their interactions, can alter the composition and properties of rocks. The main alteration minerals were quartz, calcite, alunite, epidote, hematite, illite, smectite, and chlorite. Therefore, the clay constituted a transition to a high-temperature environment, as evidenced by high temperature hydrothermal alteration minerals such as quartz (>180 °C) and epidote (~250 °C).

1. Introduction

The Republic of Djibouti is situated in the Afar depression, which is at the junction of three rifts (the Red Sea, Gulf of Aden, and East African rifts) [1]. The Italian National Research Council and the French National Center for Scientific Research conducted detailed studies of the area in the 1970s and confirmed the existence of spreading axes, similar to oceanic rifts, in Afar [2]. The landmass of Djibouti consists mainly of volcanic rocks, given the volcanism and extensive tectonism that has occurred there since 25 Ma [3]. Volcanic rocks in the region are represented by the rift-related bimodal basalt and rhyolite or trachyte suites. The series of volcanic rocks that were formed during different phases of volcanic eruption and expansion are the Adolei basalts (25 Ma), Mabla rhyolites (15 Ma), Dalha basalts (9 Ma), Ribta rhyolites (4.25 Ma), Stratoid basalts and trachytes (3.3 Ma), Gulf of Tadjoura basalts (3.1 Ma), and recent rifts basalts (Holocene to present) [4]. Phases of

extensional tectonism and related volcanism have also created numerous geothermal systems in Djibouti, characterized by medium enthalpy (>90 °C) fields with a shallow heat source provided by young rift-related volcanic rocks [5]. The most tectonically active structure in Djibouti is the Assal rift. The first geothermal exploration in Djibouti was conducted by the French Geological Survey in the 1970s [3]. The study area, Hes-Daba, is in the Gagade region of the Great East African Rift, which is currently active and opening up at a rate of 10 to 15 mm/year [6, 7].

It is important to determine the affecting criteria of the renewable energy sources for the investors as a guide [8]. Therefore, the main aims of this work were to estimate the formation temperature of Hes-Daba and evaluate its history of thermal activity and thermal structure, evaluate local geothermal systems, and understand local geothermal reservoir zones.

2. Geological Setting

Most of Djibouti is composed of Cenozoic sedimentary and volcanic rocks [9], as shown in Figure 1.

It is located at the junction of three major rifts: the continental Great East African rift, Gulf of Aden, and Red

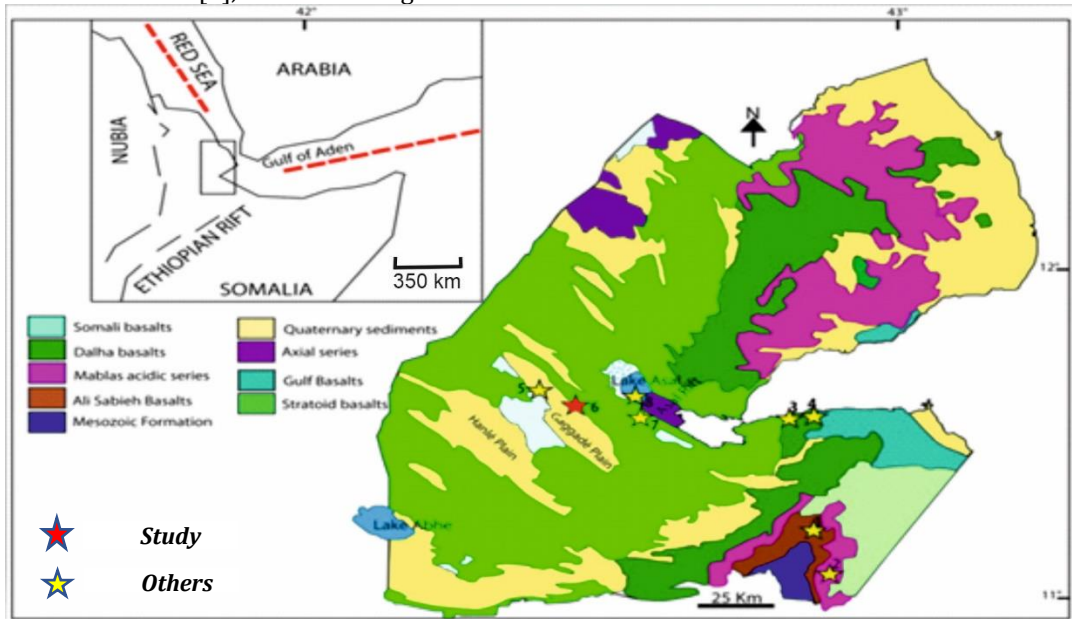


Figure 1. Geological map of republic of Djibouti (Study: Hes- Daba Geothermal Area, Others: Other Geothermal Areas in Djibouti) [8].

Sea rifts. The junction of these three rifts is located in the Afar region of Djibouti and Ethiopia [10]. This area represents a region of stretching, oceanic crust exposure, and extrusive flood basalts that preceded- rifting [11]. The Hes-Daba area is located between the Gagade and Asal faulted depressions, in one of the felsic extrusions interstratified in the intermediate member of the 3.3–1 Ma Stratoid basalt series [12]. Several parallel NW-SE trending, steeply NE-dipping normal faults transect the subhorizontal SW-dipping basaltic rocks.

Most mineralization is in a network of 2-km-long rift-parallel veins that cut through dominantly trachytic lava depositions [13].

Figure 2 shows the location of the sampling sites (H1 to H18) in the study area. Most samples were collected from quartz veins. The orientation and physical properties of the outcrop were measured in the field. These veins are texturally massive, and have thickness ranging from mm to a few cm in size and white to grey in color. Their host rocks are porphyritic trachytic rocks with feldspar (e.g. plagioclase and sanidine) and biotite phenocrysts.

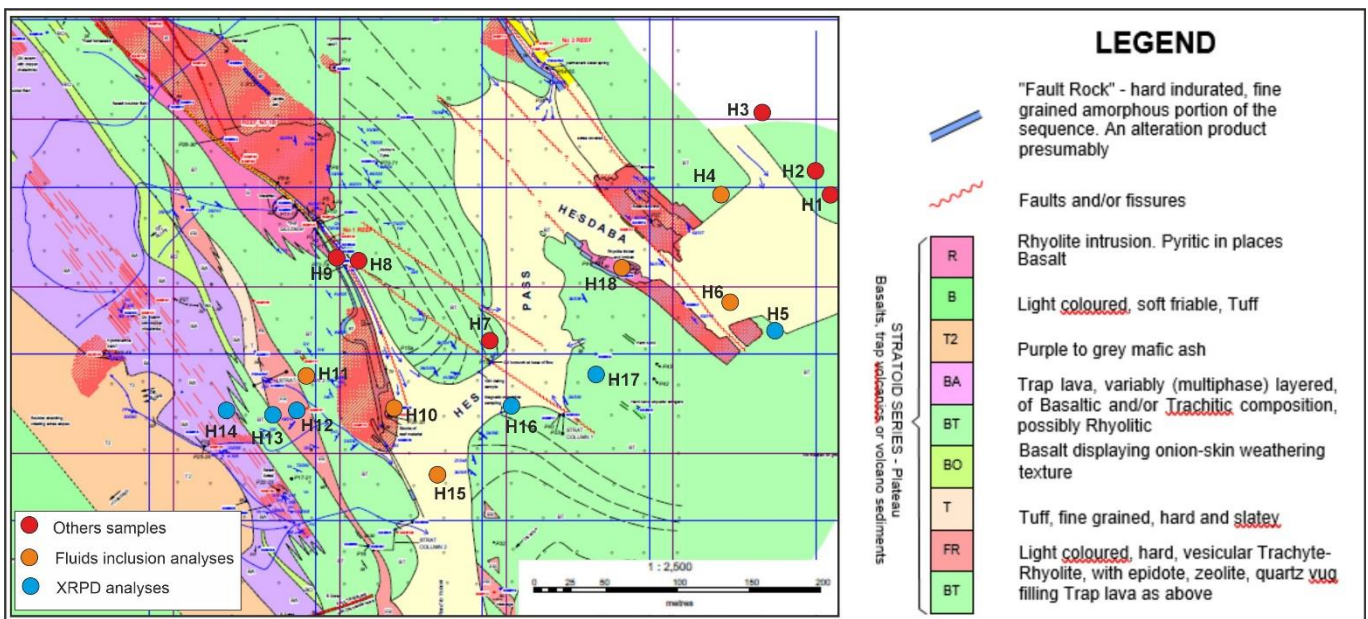


Figure 2. Location map of the samples (H5, H12, H13, H14, H16 and H17: trachytic host-rock samples, and H1, H2, H3, H4, H6, H7, H8, H9, H10, H11, H15 and H18: vein samples).

3. Method

In this study, quartz-rich vein samples hosted by trachytic rocks from the Hes-Daba geothermal area were investigated for geochemical analysis. Six trachytic host-rock samples (H5, H12, H13, H14, H16 and H17) analyzed by XRPD and two polished samples from veins (H7 and H9) were analyzed in the geological laboratory of Kyushu University.

3.1. Fluids Inclusions

Fluid inclusions are small volumes of paleofluids (liquid, gases, or solids) trapped in minerals [14]. There are two types of fluid inclusions, primary and secondary; primary inclusions occur when fluids are trapped along growth zones and crystal faces that are typically solitary or isolated [15]. These are good indicators of the crystallization conditions of host minerals [16]. Secondary fluid inclusions, however, occur when the fluids are trapped in fractures that develop after the

formation of the host mineral and thus could not escape as the former sealed [17]. The study of fluid inclusions provides key data such as the temperature, pressure, salinity, density, and chemical composition of the fluids [18].

Preparing the samples for fluid inclusion analysis needed a lot of care and time. The rock samples were polished several times with different materials (powders and discs) of different sizes. The first step was to cut the samples with an isometric cutter and then polish them until a flat surface was obtained. The samples were then glued on to a glass plate and left for 7 h to solidify. The other side of the samples are then cut and re-polished to the size of the normal thin section—which is $\sim 3 \times 5$ cm in size and typically has an ideal thickness of between 90 and 120 μm , depending on the transparency of the host crystal and the size and abundance of the inclusion—with discs and powders [19]. The size of the section is a very important factor [20]. The steps described above are shown in Figure 3.

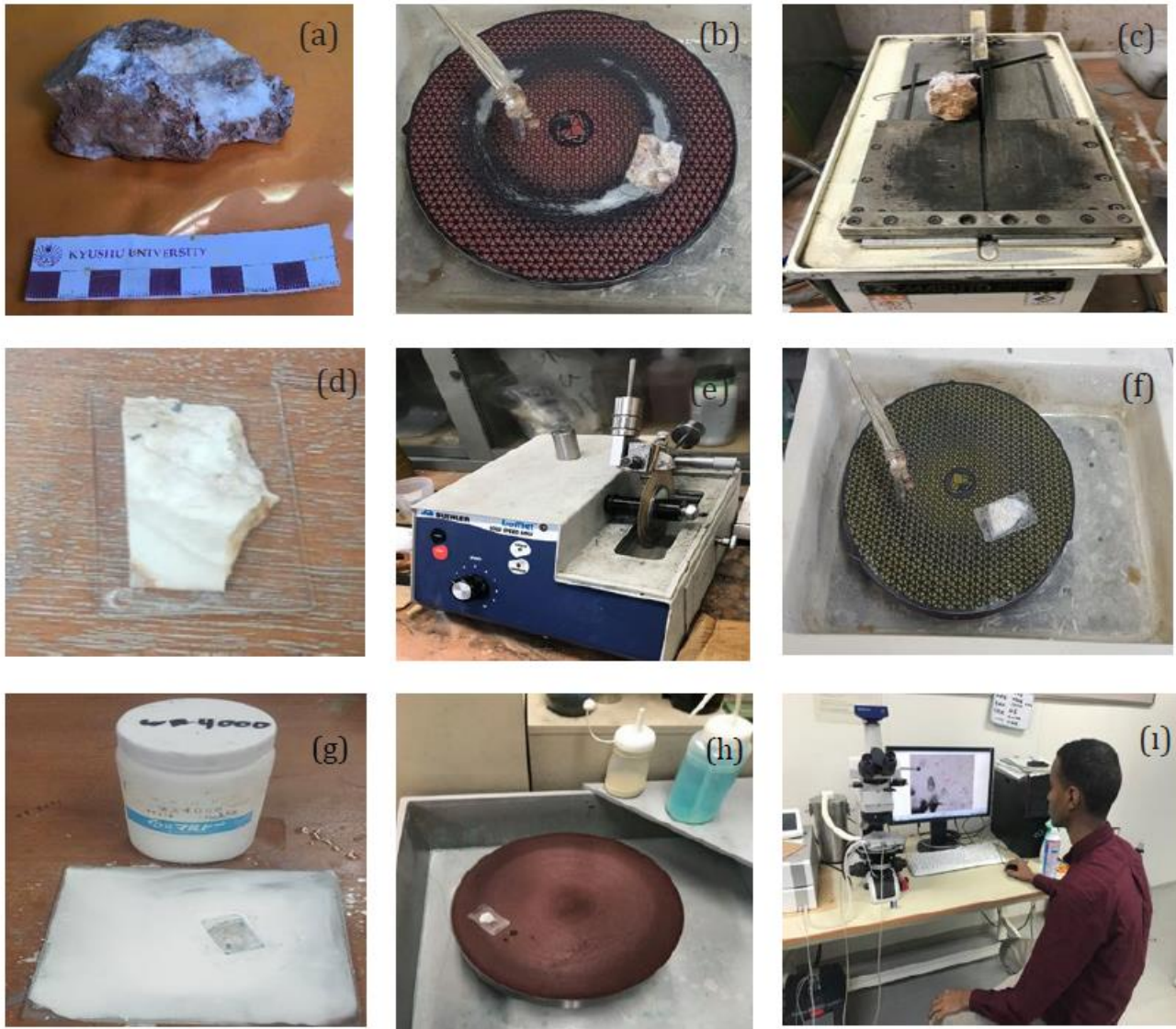


Figure 3. Fluids inclusions and instrumentation (a) rock sample, (b) polish the sample, (c) cut the sample with the cutter (d) stick the sample on the glass plate, (e) cut the sample with the isometric cutter, (f) polish the other side of the sample, (g) polish with the powder 4000, (h) diamond polish, (i) measurement of fluid inclusions microthermometry.

3.2. XRPD Analysis

X-Ray Powder Diffraction (XRPD) analysis can identify alteration minerals formed by geothermal activity [21]. The creation of alteration minerals depends on the fluid temperature, water chemistry, and composition of the host rock [22].

Two types of powdered samples bulk and oriented were prepared in a laboratory for the XRPD analysis. The objective of the bulk sample analysis was to quickly identify the constituents of the sample. To prepare the bulk sample, the rock samples were crushed into small pieces and dried in an oven at 45 °C for 1 d to remove moisture from them. The sample was then crushed into a powder. Finally, the powdered samples were compressed into a thin film on a metal plate to allow the use of XRD to properly analyze the altered minerals [23].

The oriented sample was prepared for use in identifying the clay minerals in the rock sample. Owing to the fragility of clay minerals at high temperatures, the sample was not dried in an oven. The crushed sample was then immersed in a beaker of de-ionized water and placed in an ultrasonic shaker for 30 min, after which the clay minerals were suspended in the solution. The solutes subsequently began to precipitate based on their

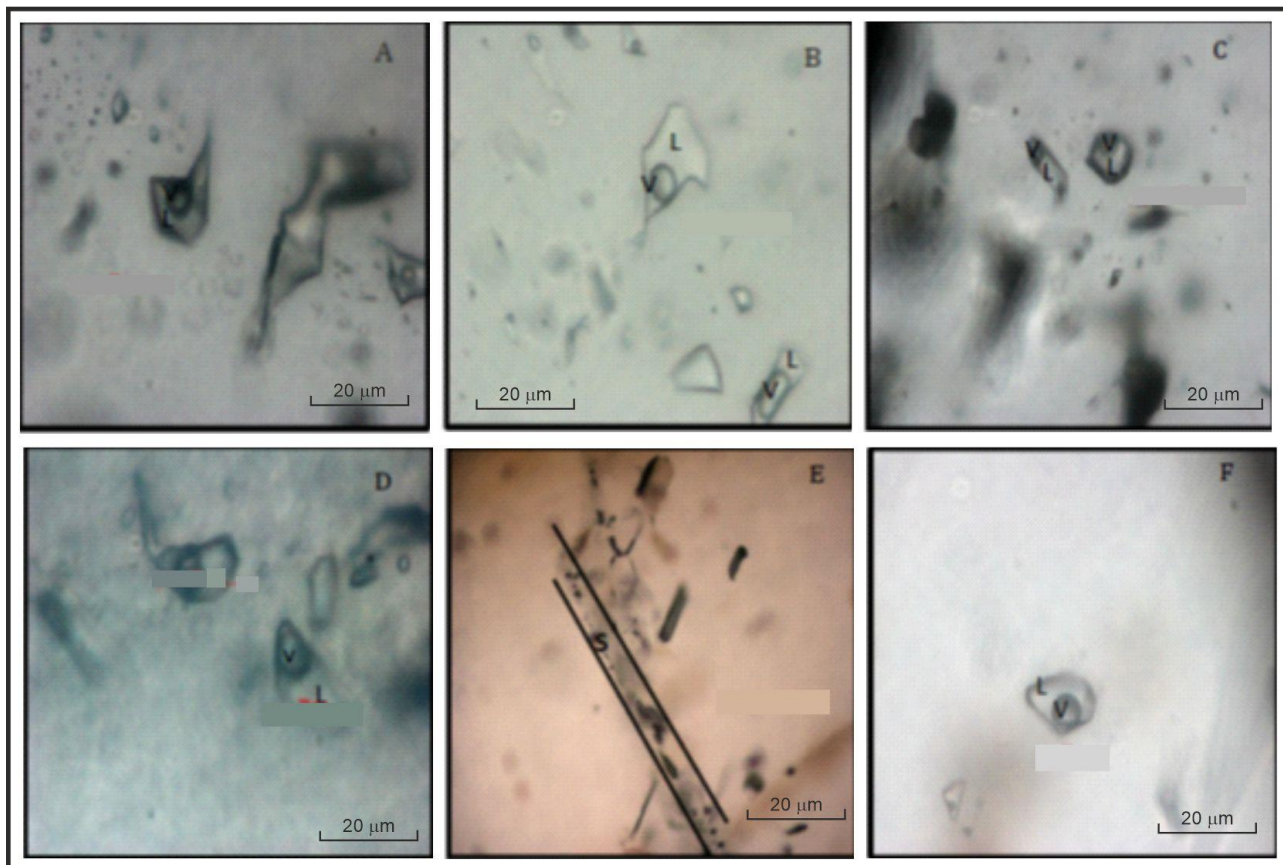
specific densities. After ~3 h, the clay minerals that appeared in the upper part of the solution were collected and centrifuged to allow collection of the concentrated clay minerals at the bottom of the tube. These clay minerals were then placed on a glass slide and air-dried for 24 h before the XRD analysis.

4. Results and Discussion

4.1. Fluids Inclusion Petrography

Figures 4A, B, C, D, and E are photographs of the fluid inclusions that were found in the sample H7, and Figure 4F shows the same for sample H9. These two samples are promising for fluid inclusion studies because there are more abundant fluid inclusions than the other samples.

The size of the inclusions varied from 10–20 μm, and most inclusions were rectangular or rectilinear; a small subset was round, appearing circular in cross-section. Two types of fluid inclusions were identified in quartz: liquid-vapor (L- V), rich in liquid and with a variable degree of filling, and vapor-liquid (V-L) rich in vapor. The most common types of inclusions were L-V and rich in liquid, with homogenization temperatures ranging from 150 °C to 367 °C.



Figures 4. Photomicrographs of fluids inclusions types quartz veins from the Hes-Daba prospect, L=Liquid and V=Vapor, primary fluid inclusion (A, B, C, D, F) and secondary fluid inclusion (E).

Figure 5 shows the frequency histograms for the homogenization temperatures of samples H7 and H9. In sample H7, there were 37 fluids inclusions; in sample H9, there were only 2. When a liquid-rich inclusion is heated, the volume of the vapor bubble decreases continuously

and smoothly with the increasing temperature until homogenization occurs. The homogenization temperature with the highest frequency in sample H7 was 225 °C.

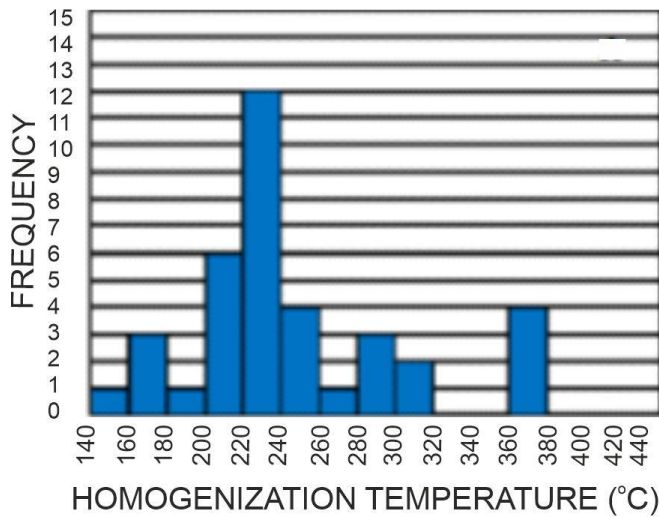


Figure 5. Frequency histograms of homogenization temperatures for fluid inclusions in quartz veins of samples, A for H7, B for H9.

The salinity of the inclusion was calculated with the freezing point depression temperature using the equation proposed by [24]:

$$\text{Salinity} = 0.00 + 1.78\varnothing - 0.0442\varnothing^2 + 0.000557\varnothing^3$$

where \varnothing is the depression of the freezing point in degrees Celsius.

Figure 6 shows relationship between the salinity and homogenization temperature for samples H2, H7, and H9. These salinities are relatively uniform and range from 0.1 wt % to 1.9 wt.% NaCl equivalent.

Primary fluid inclusions in the crystal in the quartz veins at Hes-Daba have a low melting temperature, which corresponds to low salinity of brine at temperatures ranging from 150 °C to 367 °C. The homogenization temperature of inclusions ranging from 150 °C to 367 °C require either the circulation of originally hot surface water deep underground; this might be expected if the circulation involved major faults in the underlying crystalline basement. The surface quartz vein is generally considered to have been created in the subsurface during the past [24]. However, the subsurface formation has been exposed to the surface due to the erosion that probably occurred with uplift. This is why the homogenization temperature of the fluid inclusion in the quartz vein sampled at the surface shows the temperature of the fluid trapped in the quartz in the subsurface [13]. When the spatial distribution of the homogenization temperature of the fluid inclusion at the surface is obtained, the temperature distribution and center of geothermal activity can be estimated for the past [25]. The low salinity of the solutions and the absence of CO₂ and minerals (e.g., halite) suggest that the main component of the fluid inclusion is meteoric water [26]. These results and those of a previous study [7].

suggest that two types of hydrothermal fluids contributed to inclusions this area: meteoric water and magmatic water diluted by meteoric water [27, 28].

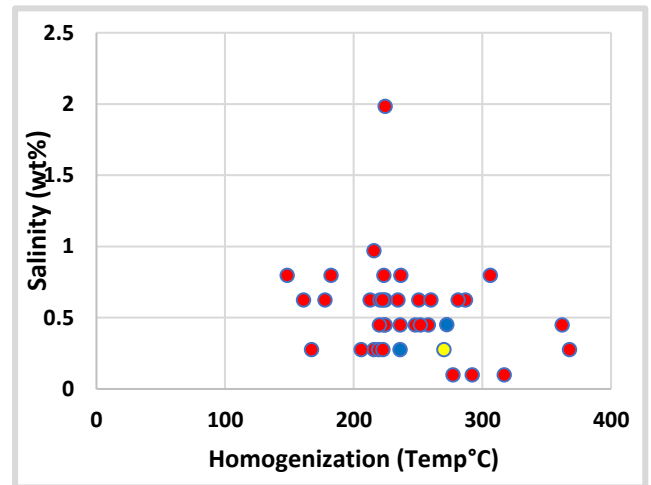


Figure 6. Salinities for fluid inclusions in quartz veins from Hes-Daba (H) and homogenization temperature for Sample H2(yellow), H7(red), and H9(blue).

4.2. XRD Results

Figure 7 shows the results of the XRD analysis of samples H5 and H12 from the trachytic host-rocks. The results are summarized in Table 1 and show that the alteration minerals in this area are mainly quartz; calcite; alunite; epidote; and the clay minerals chlorite, smectite, and illite. Quartz occurs either as an alteration product of opal or chalcedony or as a vesicle or vein filling mineral [7]. These are common and abundant minerals formed in geothermal systems and their presence in significant quantities may indicate specific temperature interval [29, 30, 31, 32, 33].

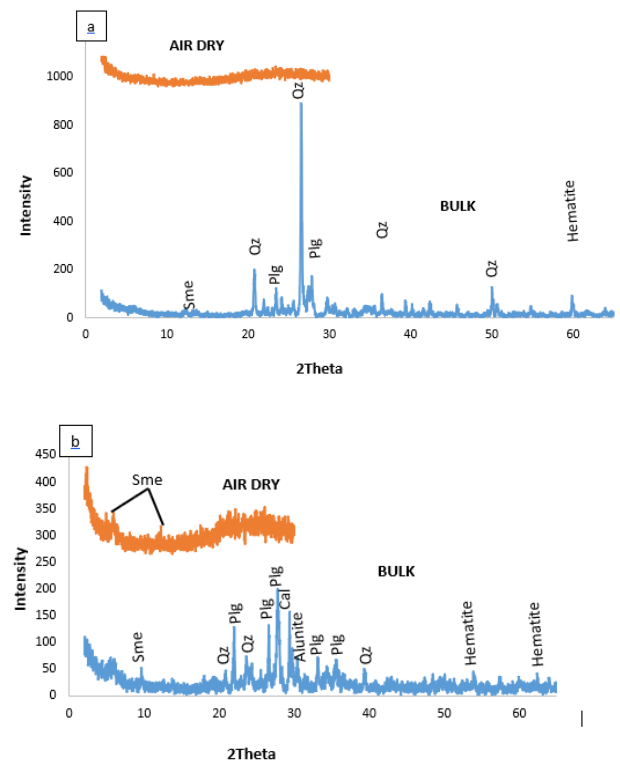


Figure 7. XRD pattern of bulk sample and oriented sample (Air-dry) a) H5 and b) H12.

These results show that the presence of clay minerals such as smectite and illite indicate that the hydrothermal alteration in this region is acidic to neutral. However, the samples containing the clay minerals (e.g. chlorite and illite) and carbonate minerals such as calcite indicate that they are neutral to alkaline. The presence of chlorite, alunite, and epidote show formation temperatures higher than 230 °C [34, 35, 36]. This temperature is inferred from Figure 8, showing the mineral stability diagram.

Table 1. Minerals identified in samples from Hes Daba.

Sample	Pl	Calcite	Quartz	Alunite	Chlorite	Vermiculite	Illite	Smectite	Hematite	Epidote
H5	xx		xx		x		x			
H12	xx	x	xx	x			x		x	
H13	xx			x				x	x	x
H14	xx		xx			x		x		
H16	xx	x	xx				x		x	
H17	xx	x			x			x	x	x

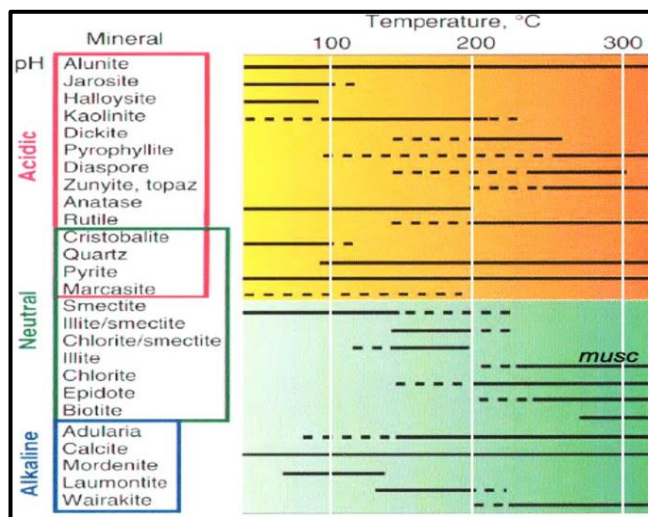


Figure 8. Variation in mineral stability with temperature at quartz solubility (dashed line for stability at amorphous silica solubility). Modified from [34].

5. Conclusion

In this study, quartz-rich vein samples hosted by trachytic rocks from the Hes-Daba geothermal area were investigated to determine temperature, salinity, and chemical composition of the hydrothermal fluids.

The primary fluid inclusions in the crystal in quartz veins from the Hes-Daba have a low melting temperature that corresponds to the low salinity of brine at temperatures ranging from 150 °C to 367 °C. The high level of salinity causes the deposition of minerals in surface areas; however, the low level of salinity in Hes-Daba means that there will be no negative effect on geothermal exploration in the area. XRPD analysis shows that the alteration minerals in this area are mainly quartz; calcite; alunite; epidote; hematite; and the clay minerals smectite, chlorite, and illite. The clay constitutes

a transition to a high-temperature environment, as evidenced by the presence of high-temperature hydrothermal alteration minerals such as quartz (>180 °C) and epidote (~250 °C). Therefore, the results XRPD analyses of fluid inclusions provide a good indication of the evolution of the geothermal system in the Hes-Daba area.

Acknowledgement

This research was financially supported by the Office Djiboutien de Développement de l'Energie Géothermique (ODDEG). We would like to thank all those who supported us in carrying out this research in Hes-Daba region. We are also grateful to the laboratories that have assisted us in the analysis of these samples. We thank Prof. Dr. Ryuichi Itoi for his contributions.

Author contributions

Ali Ferat Bayram: Conceptualization, Methodology, Software, Field study, Visualization, Investigation, Writing-Reviewing and Editing. **Moussa Hassanleh Hassan:** Data curation, Writing-Original draft preparation, Software, Validation., Field study

Conflicts of interest

The authors declare no conflicts of interest.

References

1. Choukroune, P., Francheteau, J., Auvray, L., Auzende, J. M., Brun, J. P., Sichler, B., ... & Lepine, J. C. (1988). Tectonics of an incipient oceanic rift: the Western extension of the Aden rift within the Gulf of Tadjoura, Republic of Djibouti. *Marine geophysical researches*, 9, 147-163.

2. Khaireh, A., (2012). Geothermal Development in Djibouti Republic: A Country Report. Geothermal-Energy.Org, 21-23.
3. Houssein, Bouh; Chandrasekharam, D.; Chandrasekhar, Varun; Jalludin, M. (2014). Geochemistry of thermal springs around Lake Abhe, Western Djibouti, International Journal of Sustainable Energy, 33(6), 1090-1102.
4. Corti, G., Bastow, I.D., Keir, D., Pagli, C. and Baker, E. (2015) Rift-related morphology of the Afar Depression. In, Billi, P. (ed.) Landscapes and landforms of Ethiopia. (World Geomorphological Landscapes) Dordrecht, NL. Springer, pp. 251-274.
5. Houmed, A. M., Haga, A. O., Abdilahi, S., & Varet, J. (2012, November). Proposal for new geothermal models and sites hierarchy in Djibouti Republic. In *Proceedings of the 4th African Rift Geothermal Conference. Nairobi, Kenya* (pp. 21-23).
6. Zan, L., Gianelli, G., Passerini, P., Troisi, C., Haga, A., (1990). Geothermal exploration in the Republic of Djibouti: thermal and geological data of the Hanlé and Asal areas. *Geothermics* 19, 561-582.
7. Moussa, N., Fouquet, Y., Le Gall, B., Caminiti, A.M., Rolet, J., Bohn, M., and Jalludin, M. (2012). First evidence of epithermal gold occurrences in the SE Afar Rift Republic of Djibouti. *Miner. Deposita* 47, 563-576.
8. Kantoğlu B., Düzdar Argun İ. (2023). Evaluation of renewable energy source alternatives prioritization. *Turkish Journal of Engineering*, 7(1), 01-08.
9. Deniel, C., Vidal, P., Coulon, C., Vellutini, P. J., & Pigué, P. (1994). Temporal evolution of mantle sources during continental rifting: the volcanism of Djibouti (Afar). *Journal of Geophysical Research: Solid Earth*, 99(B2), 2853-2869.
10. Gaulier, J. M., & Huchon, P. H. I. L. I. P. P. E. (1991). Tectonic evolution of Afar triple junction. *Bulletin de la Société géologique de France*, 162(3), 451-464
11. Varet, J. (2021). Relationship of the Pan-African Tectonic Structures with the Opening of the Afar Triple Junction. *The Geology of the Arabian-Nubian Shield*, 737-771.
12. Awaleh, M.O.; Boschetti, T.; Adaneh, A.E.; Daoud, M.A.; Ahmed, M.M.; Dabar, O.A.; Soubaneh, Y.D.; Kawalieh, A.D.; Kadieh, I.H. (2020). Hydrochemistry and multi-isotope study of the waters from Hanlé-Gaggadé grabens (Republic of Djibouti, East African Rift System): A low-enthalpy geothermal resource from a transboundary aquifer. *Geothermics* 86, 101805.
13. De Vivo, B. and Frezzotti, M.L. (1994). Fluid inclusions in minerals: methods and applications. Short course of the working group (IMA) "Inclusions in Minerals" Pontignano/Siena 14 Sept. 1994, Fluids Research Laboratory, Department of Geological Sciences, YPI, Blacksburg, VA, USA.
14. Randive, K. R., Hari, K. R., Dora, M. L., Malpe, D. B., & Bhondwe, A. A. (2014). Study of fluid inclusions: methods, techniques and applications. *Geological Magazine*, 29(1 and 2), 19-28.
15. Touret, J. (1977, April). The significance of fluid inclusions in metamorphic rocks. In *Thermodynamics in Geology: Proceedings of the NATO Advanced Study Institute held in Oxford, England, September 17-27, 1976* (pp. 203-227). Dordrecht: Springer Netherlands.
16. Van den Kerkhof, A. M., & Hein, U. F. (2001). Fluid inclusion petrography. *Lithos*, 55(1-4), 27-47.
17. Roedder, E. (1972). *Composition of fluid inclusions* (No. 440-JJ).
18. Parry, W. T. (1998). Fault-fluid compositions from fluid-inclusion observations and solubilities of fracture-sealing minerals. *Tectonophysics*, 290(1-2), 1-26.
19. Stoops, G. (2021). *Guidelines for analysis and description of soil and regolith thin sections* (Vol. 184). John Wiley & Sons.
20. Chaplin, I. (1998). Preparation of Thin Sections. *Microscopy Today*, 6(7), 8-9.
21. Sumotarto, U., Irawan, A., & Hendrasto, F. (2020). Study of Hydrothermal Alteration Based on Analysis of X-Ray Diffraction at Cisolak Geothermal Area, Sukabumi District, West Java. In *Proceedings World Geothermal Congress* (Vol. 1).
22. Savage, D., Walker, C., Arthur, R., Rochelle, C., Oda, C., & Takase, H. (2007). Alteration of bentonite by hyperalkaline fluids: a review of the role of secondary minerals. *Physics and Chemistry of the Earth, Parts A/B/C*, 32(1-7), 287-297.
23. Bish, D. L., Reynolds, R. C., & Post, J. E. (1989). Sample preparation for X-ray diffraction. *Modern powder diffraction*, 20, 73-99.
24. Bodnar, R.J. (1994). Philosophy of fluid inclusions analysis. In: De Vivo and M.L. Frezzotti (Eds.), *Fluid Inclusions in Minerals and Applications*. Virginia Tech, Blacksburg, VA, pp.1-6.
25. Moore, J. N., Adams, M. C., & Anderson, A. J. (2000). The fluid inclusion and mineralogic record of the transition from liquid-to vapor-dominated conditions in the Geysers geothermal system, California. *Economic Geology*, 95(8), 1719-1737
26. Roedder, E. (1963). Studies of fluid inclusions; [Part] 2, Freezing data and their interpretation. *Economic geology*, 58(2), 167-211.
27. So, C. S., Shelton, K. L., Chi, S. J., & Yun, S. T. (1991). Geochemical studies of the Gyeongchang W-Mo Mine, Republic of Korea; progressive meteoric water inundation of a magmatic hydrothermal system. *Economic Geology*, 86(4), 750-767.
28. Aydın Ertuğrul N., Hatipoğlu Bağcı Z., Lütfi Ertuğrul Ö., (2018). Aquifer Thermal Energy Storage Systems: Basic Concepts and General Design Methods. *Turkish Journal of Engineering*, 2 (2), 38 – 48.
29. Gebrehiwot M.K. (2010). Subsurface geology, hydrothermal alteration and geothermal model of Northern Skarðsmýrarfjall, Hellisheiði geothermal field, SW Iceland. University of Iceland, Faculty of Geosciences, UNU-GTP, Iceland, report 5, 65 pp.
30. Kristmannsdóttir, H. (1979). Alteration of basaltic rocks by hydrothermal activity at 100-300°C. In: Mortland, M.M., and Farmer, V.C. (editors), *International Clay Conference 1978*. Elsevier Scientific Publishing Co., Amsterdam, pp.359-367.

31. Kudo, A. M., & Weill, D. F. (1970). An igneous plagioclase thermometer. *Contributions to Mineralogy and Petrology*, 25(1), 52-65.
32. Eren M., Kadir S., and Akgöz M. (2017). Mineralogical, Geochemical and Micromorphological Characteristics of Calcite Precipitated from A Thin Cover of Recent Water Taken from The Stalagmites in K peli Cave, Esenpinar (Erdemli, Mersin), Southern Turkey. *Turkish Journal of Engineering (TUJE)*, 1 (2), 44-51.
33. Beaufort, D., Papapanagiotou, P., Patrier, P., Fujimoto, K., & Kasai, K. (2021). High temperature smectites in active geothermal systems. In *Water-Rock Interaction* (pp. 493-496). Routledge.
34. Hedenquist, J.W., Arribas, A. and Gonzales-Urien, E. (2000). Exploration for Epithermal Gold Deposits, *SEG Reviews*, 13, pp.245-277.
35. Akben, Y. B., Yal ın, C., & Uras, Y. (2023). Geology, mineralogy and geochemical signatures of carbonate-hosted Pb-Zn Deposit in margin fold belt: Dadađlı-Kahramanmaraş, T rkiye. *Engineering Applications*, 2(1), 60-68.
36. Ulu, A. E., Aydın, M. C., & Işık, E. (2022). Energy dissipation potential of flow separators placed in spillway flip bucket. *Advanced Engineering Science*, 2, 60-66.